RSC Advances

ROYAL SOCIETY OF CHEMISTRY

www.rsc.org/advances

The effect of Organomodified ZnAl LDH for *In situ* synthesis and the property of Polyethylene terephthalate Nanocomposites

Tsung-Yen Tsai, [a,b,c*] Naveen Bunekar [a,c]

[a]Department of Chemistry, Chung Yuan Christian University, [b]Master Program in Nanotechnology & [c]Center for Nanotechnology, Chung Yuan Christian University, Chung-Li District, Taoyuan City, Taiwan, Republic of China 32023.

E-mail: yen@cycu.edu.tw; Fax: +886-3-2653399; Tel: +886-3-2653342

Abstract

Polyethylene terephthalate–layered double hydroxide (PET–LDH) composites prepared by intercalation, followed by *in-situ* polymerization. To enhance the compatibility between PET and the modified LDH, sodium salt of sulfanilic acid (SAS) had been previously intercalated in the LDH. X-ray diffraction (XRD) and Transmission electron microscopy (TEM) were used to detect the degree of dispersion of the filler and the type of the polymeric composites obtained. As identified by differential scanning calorimetry (DSC) and thermogravimetric (TGA) analysis, the crystallization rate and thermal degradation temperature of the as-prepared PET nanocomposites sample were enhanced compared with pristine PET sample. The results indicated that the modified ZnAl LDH-SAS improves the interlayer compatibility between the PET and ZnAl LDH-SAS layers, thus making it easier for the oligomer to enter the gallery of ZnAl LDH-SAS layers. Hence, the polymer chains can be intercalated between the LDHs layers during the polymerization of the polymer matrix. The gas barriers, mechanical properties of these new types of PET nanocomposites were investigated.

Keywords: Polyethylene terephthalate, Layered double hydroxide, Polymerization, Crystallization, Nanocomposites.

1. Introduction

PET is hydrophobic and semicrystalline polyester due to the presence of the aromatic ring in the polymeric structure it shows high melting point and very good mechanical strength even numerous excellent properties such as good flexibility, thermal stability, fatigue resistance, high crystal-melting temperature, and low cost, etc. [1-4]. Also it has been found wide range of various applications such as in textile fibers, films, bottle containers, food packaging materials, engineering plastics in electronics, automobiles, etc. Furthermore, in recent years there is an increasing interest for the preparation of PET nanocomposites, due to their enhanced the thermo-mechanical, gas barrier and optical properties for many other applications [5-8].

The main industrial PET production is usually carried out in two stages: one is the bis (2-hydroxyethyl) terephthalate (BHET) oligomerization, and another associated with prepolymer is synthesized either through esterification of terephthalic acid (TPA) or dimethyl terephthalate (DMT) with ethylene glycol (EG). However, zinc acetate or manganese and antimony catalysts

used for polycondensation reaction but they do not provide satisfactory products, but zinc acetate or manganese catalyst are also active in ester decomposition [9, 10]. However, residual heavy-metal catalysts in PET products are harmful to the health, particularly when used in food or beverage packaging. Thus, without addition of the heavy-metal catalyst the development of a new method for the rapid polymerization of PET synthesis is desirable. Nanocomposites constitute is one of the most recent areas of nanotechnology. From technological prospect it is clear that the melt mixing process is not a preferable method for preparation of polymeric nanocomposites [11]. Due to high melt viscosity, degradation decomposition, and discoloration issues and thermodynamic restrictions, inherently effective and suitable for development of a desired morphology for some polymers. It may also lead to the production of nanocomposites with a low degree of delamination or exfoliation of inorganic nanolayers.

Fortunately, organically modified nanofillers (LDHs) provide an opportunity to solve the above mentioned problems. In general, LDHs can be applied as catalysts, photo catalysts, ion exchangers, separation science, and adsorbents, cancer therapy, polymer nanocomposites etc. [12-17]. Continuation of our research; here we developed organomodified ZnAl LDH used as a new catalyst without heavy metals to prepare new type of PET/ZnAl LDH-SAS nanocomposites by *in-situ* preparation method. The major advantage of LDHs is that their Morphology, aspect ratio can be controlled by changing the reaction conditions. The study on the LDH nanocomposites with various polymers, concerning physical properties and dispersion, has been widely reported. It also shows that PET nanocomposites synthesized via *in-situ* interlayer polycondensation process have higher degrees of LDH dispersion (intercalation/exfoliation) and hence possess enhanced physical and mechanical properties in comparison to those prepared by the melt intercalation technique. In this paper, our focus is on development of new type PET/ZnAl LDH-SAS nanocomposites. During the in situ polymer condensation nanofillers intercalated and partially exfoliated into the PET matrix resulting well dispersed PET nanocomposite formed and confirmed by WAXRD and TEM characterization. Furthermore, the thermomechanical and gas barrier properties of pristine PET and its nanocomposites, it was revealed that all samples presented a good thermomechanical and gas barrier properties as compare to pristine PET. On the side the PET/ZnAl LDH-SAS nanocomposites retain good optical properties.

2. Experimental

2.1 Materials

All the chemicals used were of analytical grade or of the highest purity commercially available. Sodium hydroxide (NaOH) were purchased from SHOWA, bis (2-hydroxyethyl) terephthalate (BHET), sulfanilic acid salt (SAS) were purchased from Sigma Aldrich. Commercial ZnAl LDH supplied from Beijing University of Chemical Technology, China, and double distilled high-purity water was obtained from the Milli-Q water (Millipore) system.

2.2 Preparation of organomodified LDHs

Commercially available ZnAl LDH calcined at 550 °C for 1 h to form Zinc–aluminum layered double oxide (LDO). After that LDO is reconstructed and modified with SAS at pH=5, Sulfanilic acid salt (SAS) (at 3 times the AEC of the Zinc–aluminum layered double hydroxide) was used as a modifier and dissolved in 50 ml of water to form a modifier aqueous solution. 2 g of LDO was then slowly added to the modifier aqueous solution, which was then placed in a high-pressure autoclave to react at 100 °C overnight with agitation to form SAS modified ZnAl LDH precipitation. The precipitation was collected by centrifugation and then washed with deionized water, followed by freeze-drying. Modified samples are designated as ZnAl LDH-SAS.

2.3 *In situ* polymerization of PET/LDH-SAS nanocomposites

Organomodified ZnAlLDHs were then blended with the bis (2-hydroxyethyl) terephthalate (BHET), and ZnAlLDH-SAS contents of the nano fillers were 0.1, 0.2, and 0.3 wt% with respect to BHET. BHET was melted at 100 °C with uniform agitation to form a mixture; the mixture was milled to form a powder. This powder was then uniformly blended with another BHET and reacted at 270°C to form a composite material of the ZnAlLDH-SAS and PET. Finally, synthesized materials are represented as PET/LDH SAS-0.1 wt%, PET/LDH SAS-0.2 wt%, and PET/LDH SAS-0.3 wt%.

3. Characterization

X-ray diffraction (XRD) was carried out on a PANalytical PW3040/60 X'Pert Pro, with Cu Kα radiation (45 kV, 40 mA) and wavelength λ=1.54 Å. The scan angle covered $2° < 2\theta < 70°$ for LDHs and nanocomposites at a scan speed of 3° min^{-1}. The morphology of PET/LDH-SAS nanocomposites was measured by scanning electron micrographs (SEM), and was obtained on a JEOL JSM 6500F. IR spectra were recorded with a JASCO, FTIR-4200 Type A spectrometer using KBr pellets. Transmission electron microscopy (TEM) images were obtained on a Model JEOL JEM2010, 200 kV. A sample with a thickness of 80 nm was prepared using a Leica Ultracut-UCT to verify the physicochemical properties of LDHs. Thermogravimetric analysis (TGA) was carried out using SII TG/DTA6200, and the experiment was performed by a 10 mg sample of PET nanocomposites under air gas flow from 40 °C to 900 °C at a scanning rate of 10 °C min^{-1}. The dynamic mechanical analysis (DMA) measurements were performed with a TA-Q800 instrument in the air at a scanning range of 40–100 °C with a heating rate of 3 °C min^{-1} with a film size of 1 cm × 4 cm (width and length) and a thickness of 80–100 mm. Gas permeability analysis (GPA) was performed with a Yanco (GTR-31). UV visible transmission and absorption spectra were obtained with a Cary-100 UV-vis spectrophotometer. Intrinsic Viscosity measured by using Ubbelohde capillary viscometer, by using following process measured the Intrinsic Viscosity (IV) and mass average molecular weight (Mw) and number average molecular weight (Mn). A solvent mixture composed of (3 wt %) phenol/ (2 wt %) 1, 1, 2, 2-tetrachloroethane was needed to prepare to dissolve PET (0.25 g) pellet in this mixture (50

ml) at 120 °C for less than 0.5 h to avoid polymer degradation. After the complete solubilization, the solutions were filtered and tested at 25 °C in water bath cylinder.

3.1.0 Results and discussion

3.1.1 Characterization of LDH and Organo-modified LDH

The commercially available ZnAl LDH and organically modified ZnAl LDH (ZnAl LDH-SAS) characterized by using XRD. The first LDH highest order of reflection was obtained 2θ at 11.4° (003), 23.5° (006) and 34.58° (009) its corresponding d spacing 7.7Å, 3.78Å and 2.54Å respectively. The diffraction near 60.67° corresponds to the (110), and 62.24° correspond to the (113) crystal planes, these indicates presence of a well ordered ZnAl LDH phase. After modification lower the 2θ value the basal spacing of (003) phase increased up to 15.34 Å. The most drastic changes in the ZnAl LDH structure are due to SAS chemically bonding with the interlayer of LDH. The changes affecting the interlayer distances and the basal spacing increase up to 7.64 Å. It is providing evidence that modifier SAS is intercalated into the galleries of LDHs, as shown in Fig. 1. The variation of d-spacing is caused by the orientation of SAS, of which the theoretical molecular sizes are 7.5 Å, it's almost equal to increased d spacing of modified ZnAlLDH. However, the shape and real intensity peaks of ZnAl LDH, modified ZnAl LDH samples have the different crystallinity. The stronger intensity of the peaks indicates a greater crystallinity of the sample. The existence of SAS polar groups and their ability to form hydrogen bonding with PET functional groups significantly improve the compatibility between the LDH and PET polymer. Further, a SEM image shows the stacked lamellar structure of ZnAlLDH, ZnAlLDH-SAS in Fig. 2(a), (b). Throughout the SEM images agglomerated particles constituted by stacked lamellar ones were seen the size decreases as the milling time is prolonged, although the shape remains unaltered. LDH platelets are not much bigger in size and the rosette crystal growth of LDH was also observed. The order of the particle size and size distributions of ZnAl LDH, ZnAlLDH-SAS is 50-150 nm, and 400-510 nm respectively.

The formation of the highly reactive modifiers was also confirmed by FTIR spectroscopy. Fig. 3 shows the FT-IR spectra of virgin LDH and the modified LDH in the region of 400-4000 cm^{-1}. SAS-modified LDHs exhibit an important number of bands, among which the most characteristic can be assigned in the following manner. Due to the presence of functional groups, a difference is observed between the FT-IR spectrum of the virgin LDH and its modified LDHs. The broad peak around 3565 cm^{-1} can be ascribed to the stretching of -OH groups attached to Zn and Al in the layers. The antisymmetric vibration of NO_3^- appears at 1385 cm^{-1}. As SAS was incorporated into the LDH interlayers, strong absorption peaks due to the aromatic compound appeared at 1633 and 1462 cm^{-1}. In addition, the peak of nitrate ion complexes, which was strongly shown in hydrotalcite, decreased significantly at around 1366 cm^{-1}, and the new peaks of sulfate ion complexes appeared at around 1032,1132, and 1160 cm^{-1} [5,7]. From the changes in these peaks, SAS anion was corroborate to be intercalated into the LDH interlayers when it was synthesized.

3.1.2 Morphology of the PET/LDH nanocomposites.

The WAXRD diagrams for the samples prepared by *in situ* polymerization are included in Fig. 4(a). For the PET-LDH series, only the PET diffraction maxima are recorded in the patterns of the composites with low LDH loading, and no reflection due to the LDH was recorded, indicating some type of disordering due to loss of the structural order of the layers. But 0.3% LDH loading showing at lower angle small peak of LDH it is evidences that intercalated morphology of PET nanocomposite. Thus, *in situ* polymerization gives rise to PET-LDH composites with well exfoliated LDH-SAS particles with low content of LDH-SAS. Such a behavior is undoubtedly related to the beneficial role played by the presence of hydrophobic modifier anions in the interlayer space, which improves the chemical compatibility with the organic polymer matrix. This could affect PET bulk properties such as thermal stability and mechanical properties.

The TEM investigations were used to corroborate the XRD results by visualizing the dispersion state of LDHs within a polymer matrix. TEM micrograph of PET/ZnAlLDH SAS-0.3 wt% nanocomposite shows in Fig. 4(b). The dark line refers to the cross-section of LDH nanolayer and the gap between two adjacent lines reveals the interlayer spacing or the LDH gallery space. The degree of delaminated platelets and dispersion of nanofiller particles are relatively low and some LDHs stacked layers still exist in the PET matrix as shown in Fig 4(b). Moreover, more LDH delaminated platelets are observed, implying the formation of more intercalated and partially exfoliated structures in PET nanocomposite in comparison with the PET sample. The TEM micrographs confirm the obtained XRD results to some extent. They clarify that the level of interchelated and partially exfoliated structures formed in PET/ZnAlLDH SAS nanocomposites.

3.1.3 Effect of organomodified LDH on Intrinsic Viscosity (IV) / Determination of molecular weight

In order to evaluate the actual effect of the nanofiller on the molecular weight of the pristine PET and PET/ZnAl LDH-SAS nanocomposites after the *in situ* synthesis, solution viscosity measurement of the pure PET and PET nanocomposites was done in order to determine the intrinsic viscosity, and an Ubbelohde viscometer was used. Based on Billmeyer and Mark-Houwink equations [18], intrinsic viscosity and the mass average molecular weight (Mw) of all samples were calculated, respectively. The Billmeyer equation is

$$[\eta] = \frac{25\times(\eta_r - 1 + 3\ln\eta_r)}{C} \qquad (1)$$

where ŋ is the intrinsic viscosity, η_r is the relative viscosity, and C refers to the concentration of pure PET or nanocomposite solutions. The obtained data were related to the number average molecular weight (Mn), Mass average molecular weight (Mw) by using the Mark-Houwink equation:

$$[\eta] = 4.68 \times 10^{-2}(\mathrm{Mw})^{0.68} \qquad (2)$$

$$[\eta] = 3.72 \times 10^{-2}(\mathrm{Mn})^{0.73} \qquad (3)$$

Therefore, after the determination of the intrinsic viscosity of all PET samples by using the solvent mixture at 25 °C, it was possible to calculate Mw of the samples by the Mark–Houwink method. The calculated results, including, intrinsic viscosities, and number average molecular weights (Mn), mass average molecular weights (Mw) of each sample, are summarized in Table 1 and Fig. 5. It may be observed that by addition of small percentages of different LDH particles to the system, the intrinsic viscosity and Mn are significantly increased as compared with that of the pristine PET [19, 20]. This observation is finding where by the more LDH that is introduced into the PET process, the greater the increase in molecular weight of the PET nanocomposite. The findings in the current work verify that the addition of nanofiller layer particles probably causes increasing the chain length for the *in situ* interlayer polymerization and as a result longer the polymer chains with higher molecular weights are formed. This effect could be attributed to the better thermal stability of PET and the suppressions of thermal decomposition reactions that take place during PET synthesis. Also, a possible increase of the heat conductivity of the polymerization mixture, due to the presence of the inorganic filler, could also contribute to the observed trend.

3.1.4 Thermal property and crystallization behavior of PET/LDH nanocomposites

As was determined earlier, the interlayer modifier affects the dispersion degree of nanolayers and hence, they may alter the thermal behavior of the synthesized nanocomposites as well. The thermal stability and decomposition of the prepared PET nanocomposite hybrids were evaluated by determining their weight loss via analysis by TGA. TGA curves for PET and PET/LDH nanocomposites with 0.1, 0.2, and 0.3 wt% of PET intercalated LDHs are shown in Fig. 6, and the results are summarized in Table 2. From the data presented in Table 2/Fig. 6, it is evident that decomposition of PET takes place in three steps. The first weight loss starts at about 300 °C, corresponds to removal of water. This second step is attributed to the partial decomposition of the polymer weight loss starts at about 400 °C. Finally, a new weight loss, due to oxidative elimination of the carbonaceous residue derived from the initial polymer degradation, is recorded at 470 °C, and all the samples are finally lost at 520 °C. In fact, LDH nanoparticles exhibit a shielding effect on the polymeric matrix. This shielding effect basically rises from the formation of the charred surface that hinders the release of evolved gases during thermal decomposition. As a consequence of the modification process, the higher exfoliated LDH platelets in PET nanocomposites act as efficient thermal barriers by formation of more tortuous paths within the PET matrix and thus increase the thermal stability of the nanocomposite. The temperature at 5% (T_{5d}) weight reduction of PET/LDH nanocomposites higher than those of pure PET. It indicates that there is a strong interaction between the PET-LDHs and polymer matrix. The exfoliated/intercalated nanolayers of PET/LDH obstructed the internal diffusion of intense heat and various gaseous substances that formed during pyrolysis of PET.

PET is a semi-crystalline polymer with a low crystallization rate, and any improvement in PET crystallization behavior, in turn, would be beneficial for its mechanical and barrier properties. Therefore, it is important to study the crystallization behavior of PET/LDH nanocomposites. Fig. 7 (a) and (b) are the differential scanning calorimetry (DSC) thermograms of pure PET and PET nanocomposites with 0.3, 0.2 and 0.1 wt% loaded modified LDHs with the heating and cooling measurements, respectively. Different thermal characteristic parameters were measured the results are listed in Table 2. The values of the melting peaks (Tm) and the glass-transition temperature (Tg) of all the nanocomposites were nearly identical regardless of the modified LDH, Indicating that the crystal structure of the PET matrix was unchanged after the formation of nanocomposites.

3.1.5 Mechanical Properties of PET/LDH nanocomposites

The DMA result of the neat PET and PET based nanocomposites are reported in Fig. 8. The incorporation of LDHs into the PET matrix increases the storage modulus and leads to more brittleness in comparison with the neat PET films. The storage modulus of the PET matrix is around 1469 Mpa, while 0.3 wt% loaded LDH platelets have a modulus of 2092 Mpa. Therefore, the presence of LDH particles within the PET matrix increases the mechanical properties because a significant portion of the applied load may be carried by the modified LDH particles. This enhancement of the modulus was ascribed to the high resistance exerted by the LDH. Furthermore, the increased stretching resistance of the polymer chains produced by the orientation of their backbones in the galleries also contributed to the enhancement of the modulus. In a polymer/LDH hybrid in which the polymer chains are restricted in mobility make significant contributions to a hybrid's tensile modulus. Thus, increasing the LDH content increases the restriction of the polymer chains mobility and results in an increase in the tensile modulus. It was discussed earlier that the polymer composites exhibited a mix of intercalated structure and dispersed tactoids. This morphology has a significant effect on the reinforcement efficiency. A stack of platelets including organomodifier or polymer chains between LDH layers can be considered as a lower effective aspect ratio and higher volume fraction.

3.1.6 Gas barrier and Optical Properties of PET/LDH nanocomposites

Permeability of packaging films is the common parameter determined to assess their mass transfer barrier property. Impermeable LDH nanolayers block gases transport through a polymer matrix, and by creating a tortuous pathway force the permeant to travel longer diffusive path. Hence, higher level of intercalated is favorable for barrier properties enhancement [21]. Thus, nanocomposites are multiphase systems in which the coexistence of phases with different permeabilities can cause complex transport phenomena. The permeability of gases through a polymer matrix depends on the available free volume of the matrix. Morphology and microstructure of these multi-phase systems are expected to play a very important role in determining the transport phenomena. In Table 3 summarized the nitrogen, oxygen and corbondioxide permeability values of the neat PET and PET-based nanocomposite films. All

nanocomposite films exhibit higher barrier properties than the neat PET due to the presence of LDH layers and larger crystal content, which can be attributed to the better LDH dispersion. Overall, PET/ZnAl LDH-SAS-3 wt% sample improvement in barrier properties was obtained for the PET nanocomposites containing modified LDH in comparison to the neat PET films. The gas permeability is calculated as

$$P = \frac{q \times k' \times l}{a \times t \times p} \left(\frac{cm^3\ cm}{cm^2 \sec\ cm\ Hg}\right) \qquad (4)$$

where q is the permeation amount, $k'$is the coefficient, l is the thickness, p is the pressure, a is the permeation area and t is the measurement time [22].

UV–Visible spectroscopy was performed in the wavelength range 200–800 nm at room temperature for the pristine PET and PET/LDH nanocomposites and the respective spectra shown in Fig. 9. A shift of the high and identical transmission ability in the visible range was observed for the PET substrate. The average transmission of the PET substrate in the visible range is about 99%. Nanocomposites results from large aspect ratio of the LDHs, which provide the reflection of the UV light, and a good dispersion of the LDH platelets, which increase the UV-light pathway in the PET matrix. Further, this type of transition occurs in compounds containing non bonding electrons and also in aromatic compounds due to bond cleavage and reconstruction. The high transmission in the visible range makes this PET substrate suitable and useful such as optoelectronic and other thin film applications.

4. Conclusion

In PET/ZnAl LDH-SAS nanocomposites were synthesized by using the *in situ* polymerization method. During the *in situ* condensation nanofillers play a critical role to form nanocomposite. Due to their dispersion in mainly intercalated and partially exfoliated arrangement into the PET matrix, much higher surface was available to interact with PET as confirmed by WAXRD and TEM characterization. DSC measurements indicate that the LDH nanofiller can act as an efficient nucleating agent for PET crystallization. Furthermore, the thermomechanical and gas barrier properties of pristine PET and its nanocomposites with ZnAl LDH-SAS prepared in situ, it was revealed that all samples presented a good thermomechanical and gas barrier properties as compare to pristine PET. On the side the PET/ZnAl LDH-SAS nanocomposites retain good optical properties.

Acknowledgement

The authors are grateful to the Ministry of Economy Affairs of Taiwan and the National Science Council of Taiwan under Grant no. MOST104-2113-M-033-007, Dr J. M. Yeh is gratefully acknowledged for assistance with the CO_2 gas barrier measurements.

References

1. L. Tammaro, V. Vittoria, V. Bugatti, Dispersion of modified Layered Double Hydroxides in Poly (ethylene terephthalate) by High Energy Ball Milling for Food Packaging applications, European Polymer Journal, 2014, 52,172-180.

2. C. I. W. Calcagno, C. M. Mariani, S. R. Texeira, R. S. Mauler, The effect of organic modifier of the clay on morphology and crystallization properties of PET nanocomposites, Polymer, 2007, 362, 966–74.

3. M. Tarameshlou, S-H. Jafari, H. Ali Khonakdar, A. Fakhravar, and M. Farmahini-Farahani, PET-based Nanocomposites Made by Reactive and Remodified Clays, Iranian Polymer Journal, 2010, 19, 19521-529.

4. M. Yin, C. C. Li, G. H. Guan, X. P. Yuan, D. Zhang, Y. N. Xiao, In-situ synthesis of poly(ethylene terephthalate)/ clay nanocomposites using TiO_2/SiO_2 sol intercalated montmorillonite as polycondensation catalyst, Polym Eng Sci, 2009,49,1562-1572.

5. T-Y. Tsai, B. Naveen, W-C. Shiua and S-W. Lu, An advanced preparation and characterization of the PET/MgAl-LDH nanocomposites, RSC Adv, 2014, 4, 25683-25691.

6. A. M. Youssef, T. Bujdosó, V. Hornok, S. Papp, A. F. A. Hakim and I. Dékány, Structural and thermal properties of polystyrene nanocomposites containing hydrophilic and hydrophobic layered double hydroxides, Appl Clay Sci, 2013, 77–78, 46–51.

7. T-Y. Tsai, J-R. Laio, B. Naveen, Preparation and Characterization of PET/LDH or Clay Nanocomposites through the Microcompounding Process, J Chin Chem Soc, 2015, 62, 547-553.

8. A. Ghanbari, M. C. Heuzey, P. J. Carreau, M. T. Ton-That, A novel approach to control thermal degradation of PET/organoclay nanocomposites and improve clay exfoliation, Polymer, 2013, 54,1361-1369.

9. L. Guihe, F. Zhifeng and C. Ding, Study on the Synthesis and properties of PET using hydrotalcite as catalyst, China Pet. Process Petro chem Technol, 2013, 15, 65-69.

10. H. Gorzawski, W. F. Hoelderich, Transesterification of methyl benzoate and dimethyl terephthalate with ethylene glycol over super bases, Appl Catal A: Gen, 1999, 179, 131-137.

11. M. C. Costache, M. J. Heidecker, E. Manias, C. A. Wilkie, Preparation and characterization of poly(ethylene terephthalate)/clay nanocomposites by melt blending using thermally stable surfactants, Polym Adv Technol, 2006,17,764-771.

12. T-Y. Tsai and W-C. Shiu, Synthesis and Characterization of Poly (ethylene terephthalate) /Modified Lithium-Aluminum-Layered Double Hydroxide Nanocomposites Prepared Using In-situ Polymerization, J Chin Chem Soc, 2014, 61, 891-896.

13. Hongmei He, Hongliang Kang, Shulan Ma, Yongxiang Bai, Xiaojing Yang, High adsorption selectivity of ZnAl layered double hydroxides and the calcined materials toward phosphate, Journal of Colloid and Interface Science, 2010, 343, 225–231.

14. T. Cao, K. Xu, G. M. Chen, C-Y. Guo, Poly (ethylene terephthalate) nanocomposites with a strong UV-shielding function using UV-absorber intercalated layered double hydroxides, RSC Adv, 2013, 3, 6282-6285.

15. Jun Liu, Guangming Chen, Jiping Yang, Preparation and characterization of poly(vinyl chloride)/layered double hydroxide nanocomposites with enhanced thermal stability, Polymer, 2008, 49, 3923-3927.

16. V. H. Giang Phan, Eunhye Lee, Jin Hee Maeng, Thavasyappan Thambi, Bong Sup Kim, Donheang Lee, Doo Sung Lee, Pancreatic cancer therapy using an injectable nanobiohybrid hydroge, RSC Adv, 2016,6, 41644-41655.

17. Ziqiao Hu, Guangming Chen, Novel Nanocomposite Hydrogels Consisting of Layered Double Hydroxide with Ultrahigh Tensibility and Hierarchical Porous Structure at Low Inorganic Content, Adv Mater, 2014, 26, 5950-5956.

18. N.B. Sanches, M. L. Dias, E. B. A. V. Pacheco, Comparative techniques for molecular weight evaluation of poly (ethylene terephthalate) (PET), Polym Test, 2005, 24, 688-693.

19. A. A. Vassiliou, K. Chrissafis, and D. N. Bikiaris, In situ prepared PET nanocomposites: Effect of organically modified montmorillonite and fumed silica nanoparticles on PET physical properties and thermal degradation kinetics,Thermochim Acta, 2010, 500, 21-29.

20. T. U. Patro, D. V. Khakhar, and A. Misra, Phosphonium-based layered silicate-Poly (ethylene terephthalate) nanocomposites: Stability, thermal and mechanical properties, J Appl Polym Sci, 2009, 113, 1720-1732.

21. S. Bhattacharya, R. Gupta, M. Kamal, Polymeric nanocomposites: theory and practice. Hanser Gardner Publications; 2007.

22. E. L. Cussler, S. E. Hughes, W. J. Ward and R. J. Aris, Barrier membranes, J Membr Sci, 1988, 38,161-174.

Figures and Captions

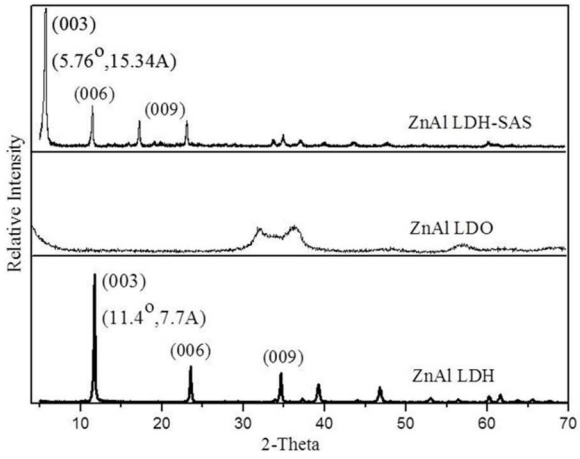

Figure 1. XRD patterns of Pure ZnAl LDH and Organomodified ZnAl LDH

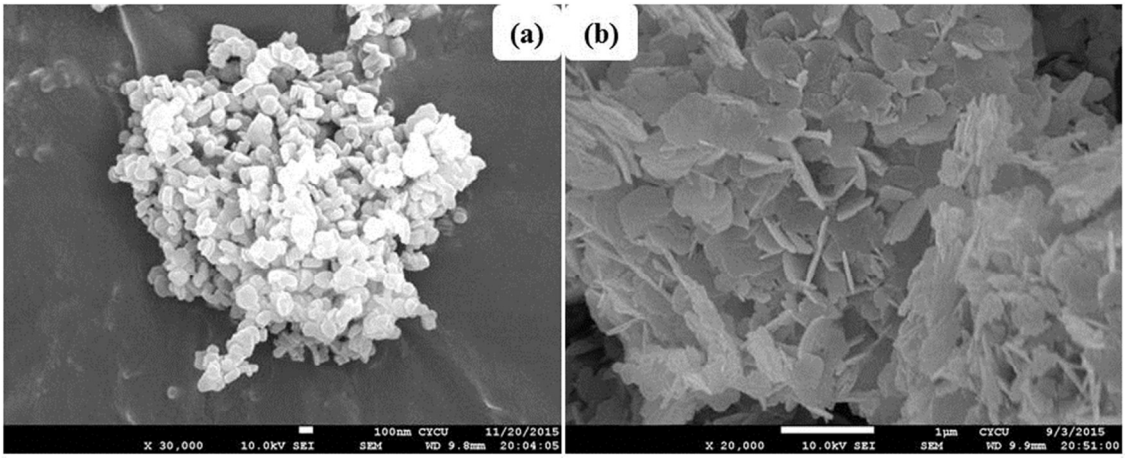

Figure 2. SEM images of (a) Pure ZnAl LDH (b) Organomodified ZnAl LDH.

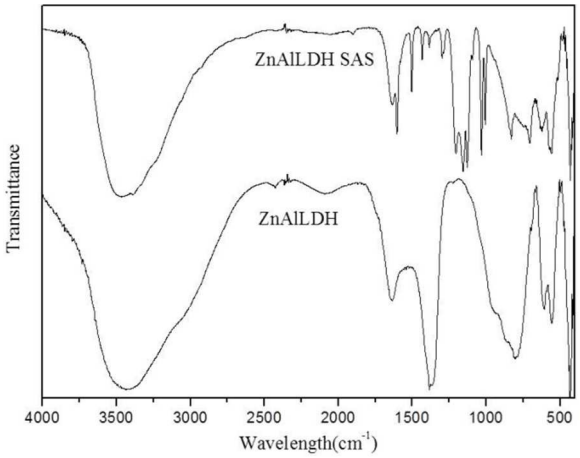

Figure 3. FT-IR spectra of Pure ZnAl LDH and Organomodified ZnAl LDH.

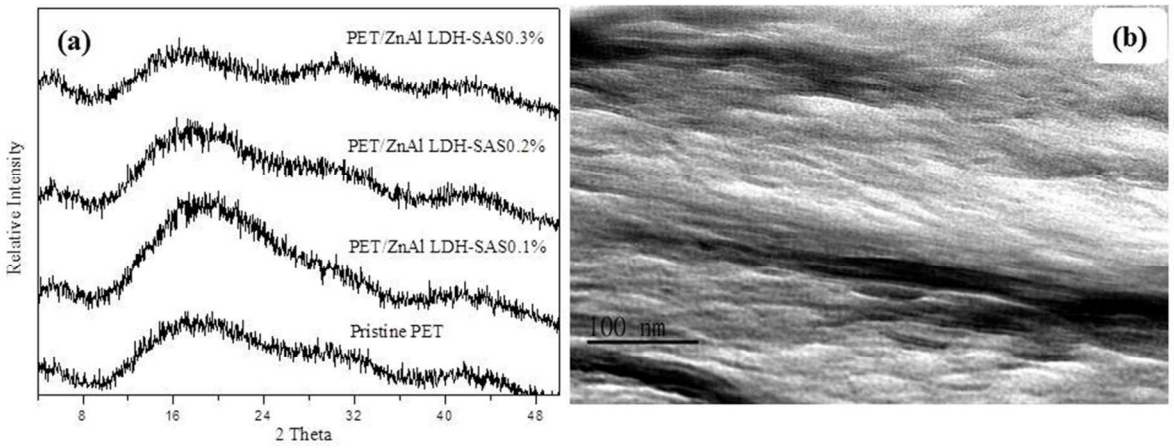

Figure 4. Dispersion morphologies of PET/ZnAl LDH-SAS nanocomposites (a) XRD Pattern (b) TEM image of PET/ZnAlLDH-SAS-0.3%.

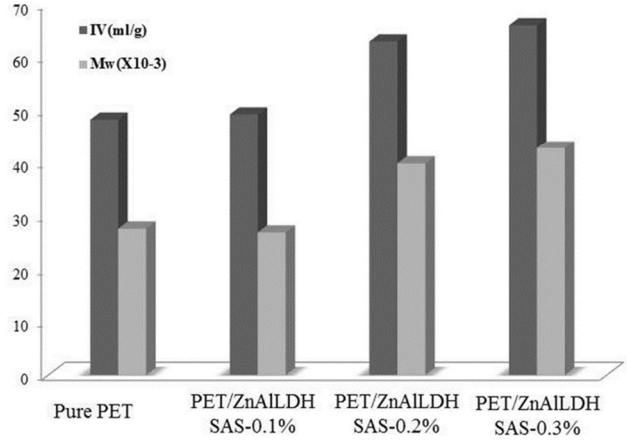

Figure 5. Viscosity and Molecular weight of polymer matrix influenced by ZnAlLDH-SAS.

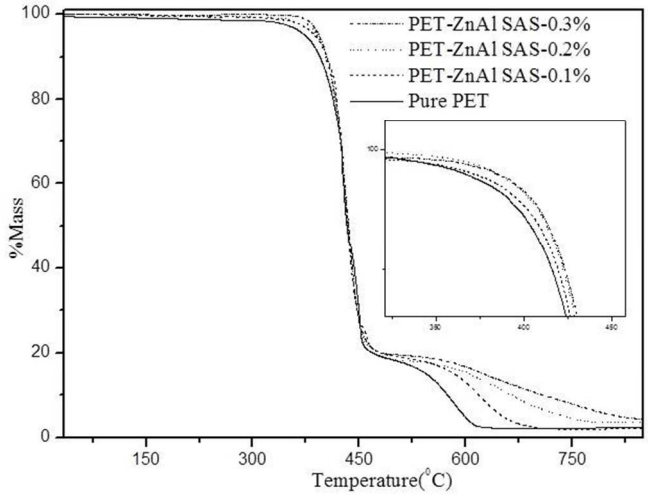

Figure 6. TGA graphs of PET/ZnAlLDH-SAS Nanocomposites.

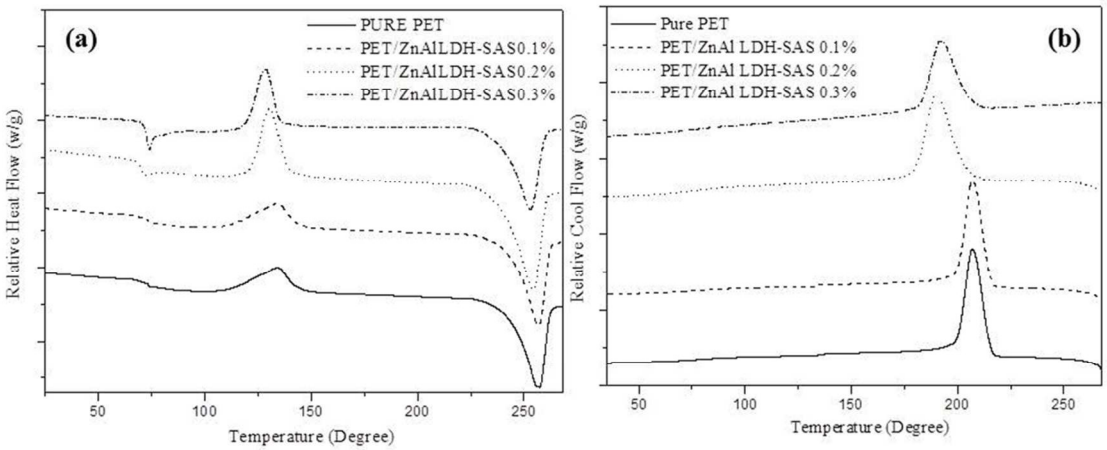

Figure 7. DSC patterns of synthesized hybrids: (a) cooling curves, and (b) heating curves

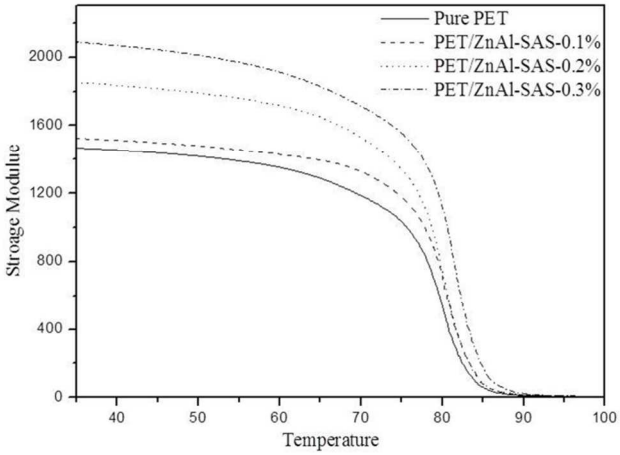

Figure 8. DMA graphs of PET/ZnAlLDH-SAS Nanocomposites.

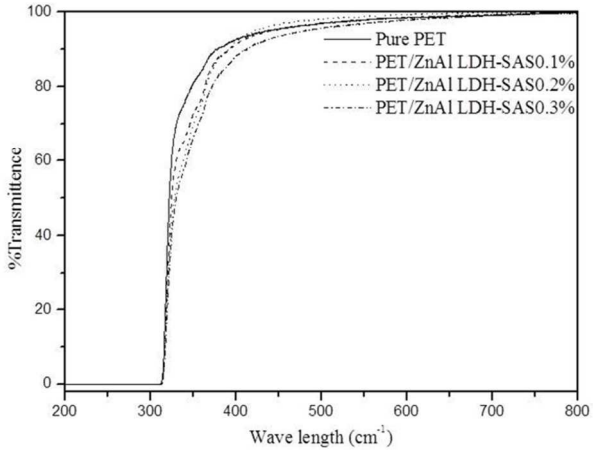

Figure 9. UV graphs of PET/ZnAlLDH-SAS Nanocomposites

Table1. Intrinsic viscosity (IV) mass average molecular weight, and number average molecular weight of synthesized PET and PET-LDH hybrids.

Sample	IV(ml/g)	Mn	Mw
Pure PET	49.09	18800.68	27653.79
PET/ZnAl SAS-0.1%	48.26	18385.65	26951.94
PET/ZnAl SAS-0.2%	62.98	26479.41	39865.32
PET/ZnAl SAS-0.3%	66.00	28230.12	42787.87

Table 2. TGA, DSC and DMA data of synthesized hybrids and pure PET.

Sample	T_{5d}	Tm	Tcc	Storage modulus(Mpa)
Pure PET	385.54	256.8	206.5	1469
PET/ZnAl-SAS-0.1%	387.72	256.4	206.5	1678
PET/ZnAl-SAS-0.2%	387.92	254.2	192.2	1859
PET/ZnAl-SAS-0.3%	392.82	252.9	189.6	2092

Table 3. Gas barrier and optical properties data of synthesized hybrids and pure PET.

	Barrier						Visible	
Sample	O_2	BIF	N_2	BIF	CO_2	BIF	550nm	800nm
Pure PET	0.42899	1.00	0.0388	1.00	0.116	1.00	98.87	100.0
PET/ZnAl-SAS-0.1%	0.30758	1.39	0.0360	1.07	0.060	1.93	98.01	99.94
PET/ZnAl-SAS-0.2%	0.27049	1.58	0.0298	1.30	0.057	2.03	97.97	99.94
PET/ZnAl-SAS-0.3%	0.15197	2.82	0.0282	1.37	0.047	2.47	97.05	99.86

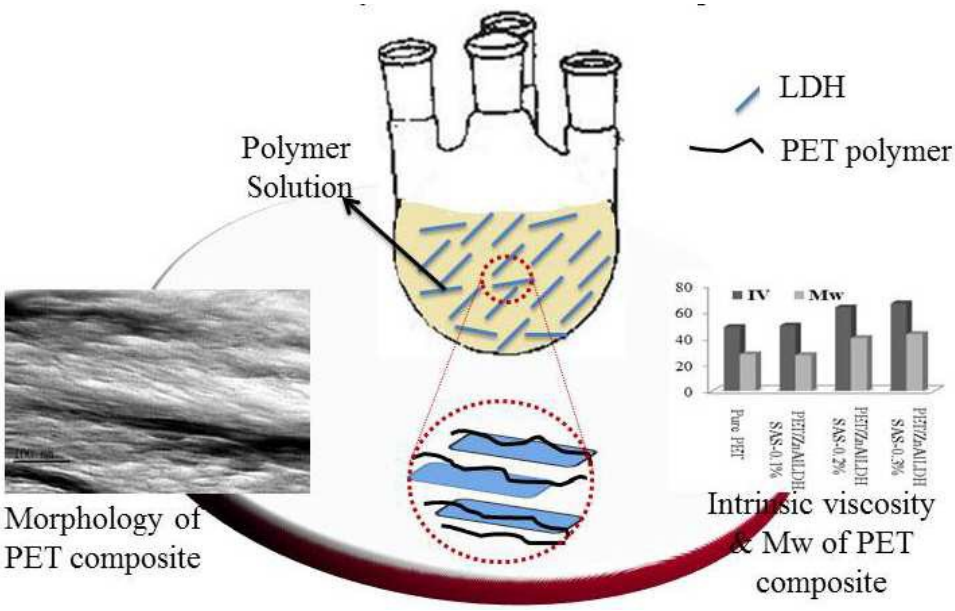

Scheme: Graphical representation of PET/ZnAl -SAS Nanocomposite *in situ* synthesis and its properties.